Water Research 208 (2022) 117855

Contents lists available at ScienceDirect

Water Research

journal homepage: www.elsevier.com/locate/watres

Effect of ultrasonication on waste activated sludge rheological properties and process economics

M. Ruiz-Hernando [a,*], S. Vinardell [a], J. Labanda [a,b], J. Llorens [a,b]

[a] Department of Chemical Engineering and Analytical Chemistry, University of Barcelona, Barcelona 08028, Spain
[b] Water Research Institute, University of Barcelona, Barcelona 08028, Spain

ARTICLE INFO

Keywords:
Waste activated sludge
Ultrasound treatment
Rheology
Thixotropic model
Dewatering
Techno-economic analysis

ABSTRACT

The present study provides an overall view of the effect of the ultrasound treatment on waste activated sludge (WAS) rheological and dewatering properties as well as its impact on the economic balance of a theoretical wastewater treatment plant. The results showed that ultrasonication at 27,000 kJ/kg TS increased the soluble protein concentration (> 100%), bound water content (~25%), and capillary suction time (> 100%) of WAS. The molecular weight distribution of the extracellular polymeric substances (EPS) revealed that the ultrasound treatment solubilised a portion of the peptides and low-molecular-weight proteins. The thixotropic behaviour of the WAS was analysed by means of a rheological structural model that defines the time evolution of a structural parameter as a function of kinetic coefficients for the breakdown and build-up processes. The ultrasound treatment reduced the kinetic coefficients for the breakdown process and changed the fast speed of alignment of flocs because of the reduction of WAS structures. Similarly, the creep tests revealed that the ultrasound treatment at 27,000 kJ/kg TS reduced the initial elasticity (~80%) and the zero-shear rate viscosity (~60%), which means that the internal structure of the WAS loosened and disrupted. Finally, a techno-economic analysis showed that ultrasonication was not yet economically favourable since its implementation increased 14% the net cost for WAS treatment and disposal. However, a sensitivity analysis illustrated that increasing electricity revenue and reducing biosolids disposal costs through improvement in WAS biodegradability is important to make ultrasound implementation economically attractive.

1. Introduction

Wastewater treatment processes produce huge amounts of both primary and waste activated sludge (WAS) (Appels et al., 2008). WAS is produced biologically and contains less organic contaminants and higher nutrients concentration than primary sludge (Radjenović et al., 2009; Weemaes and Verstraete, 1998). However, WAS is difficult to dewater compared with primary sludge due to the existence of colloidal materials and extracellular polymeric substances (EPSs) (Houghton and Stephenson, 2002). The sludge floc matrix is represented by a dynamic double-layered EPS structure (Li and Yang, 2007) with tightly bound EPSs (TB-EPSs) located in the inner layer and loosely bound EPSs (LB-EPSs) located in the outer layer (Sheng et al., 2010). Accordingly, LB-EPSs may function as the primary surface for cell attachment and flocculation (Li and Yang, 2007). Additionally, WAS is primarily formed by microorganisms and therefore more difficult to digest under anaerobic conditions due to the presence of glycan strands in microbial cell walls (Appels et al., 2008).

Several pre-treatments have been proposed in the literature to improve the digestibility and dewaterability of WAS, such as ultrasound (Lippert et al., 2021), thermal (Ruiz-Hernando et al., 2015b), alkaline (He et al., 2021) and freezing combined with nitrite addition (Liu et al., 2020). Ultrasound, which can partially disintegrate the WAS by disrupting flocs and solubilising the EPSs, is one of the most researched techniques for WAS pre-treatment (Bandelin et al., 2020; Feng et al., 2009). The ultrasound disintegration mechanism is based on the cavitation phenomenon, which is the formation, growth and violent collapse of cavitation bubbles, caused by alternate compression and rarefaction cycles of ultrasound waves travelling through the WAS (Gallipoli and Braguglia, 2012). This violent collapse generates powerful hydro-mechanical shear forces in the bulk liquid surrounding the bubbles. The ultrasound range is divided in three regions depending on the frequency: (i) power ultrasound (20–100 kHz), (ii) high frequency ultrasound (100 kHz–1 MHz), and (iii) diagnostic ultrasound (1–500 MHz) (Pilli et al., 2011). According to Carrère et al. (2010), low frequencies

* Corresponding author.
E-mail address: maria.ruiz@ub.edu (M. Ruiz-Hernando).

https://doi.org/10.1016/j.watres.2021.117855
Received 12 August 2021; Received in revised form 24 October 2021; Accepted 5 November 2021
Available online 10 November 2021

Nomenclature

E_S	Ultrasound specific energy (kJ/kg TS)
P	Ultrasonic power of the ultrasonic homogeniser (kW)
t_a	Application time for the ultrasound treatment (s)
V	Sample volume for the ultrasound treatment (L)
$\gamma(t)$	Time-related strain (-)
τ_a	Applied shear stress (Pa)
$J(t)$	Time-related compliance (Pa^{-1})
J_0	Instantaneous elastic compliance of the Maxwell spring (Pa^{-1})
λ	Relaxation time (s)
J_m	Viscoelastic compliance associated to the mean λ of the Kelvin–Voigt element (Pa^{-1})
η_0	Zero-shear rate viscosity of the Maxwell dashpot (Pa·s)
G_0	Initial elasticity (Pa)
a	Consistency index ($Pa{\cdot}s^n$)
n	Power law index (-)
K	Thixotropic kinetic coefficient (s^{-1})
K_{down}	Thixotropic kinetic coefficient for the breakdown process (s^{-1})
K_{up}	Thixotropic kinetic coefficient for the build-up process (s^{-1})
α_{down}	Alpha kinetic parameter for the breakdown process ($s^{\beta down-1}$)
β_{down}	Beta kinetic parameter for the breakdown process (-)
α_{up}	Alpha kinetic parameter for the build-up process ($s^{\beta up-1}$)
β_{up}	Beta kinetic parameter for the build-up process (-)
S	Structural parameter ($Pa{\cdot}s^{1-m}$)
S_e	Steady state structural parameter ($Pa{\cdot}s^{1-m}$)
S_i	Initial structural parameter when a shear rate is applied ($Pa{\cdot}s^{1-m}$)
t	Shear time (s)
$\dot{\gamma}$	Shear rate (s^{-1})
m	Parameter that quantifies the instantaneous alignment and deformation of sludge flocs (-)
η	Viscosity (Pa·s)
η_e	Steady state viscosity (Pa·s)
η_i	Initial viscosity when a shear rate is applied (Pa·s)

(20–40 kHz) are the most efficient in sludge treatment.

Rheology is a useful tool for the characterisation of sludge suspensions. Two major types of rheological measurements can be distinguished: (i) those perform within the linear viscoelastic region and (ii) those perform within the non-linear viscoelastic region (Ruiz-Hernando et al., 2014b). When performing rheological measurements within the linear viscoelastic region, the analysed material flows with its original structure unchanged due to the low shear stresses applied. The linear viscoelastic properties can be measured using the creep test, in which a constant stress in the linear viscoelastic region is applied and the time-related strain is measured (Farno et al., 2020). Conversely, when rheological measurements are performed within the non-linear viscoelastic region, the material flows with the application of moderate or high shear stress. Under these conditions, elasticity is notably reduced and viscosity governs the rheological behaviour of WAS, being dependent on the applied shear rate (Labanda and Llorens, 2006).

Under steady state laminar flow, WAS generally behaves as a non-Newtonian pseudoplastic fluid (Ratkovich et al., 2013). According to the literature, the Ostwald–de Waele model is the most commonly used equation to represent the non-Newtonian behaviour of sludge because of its simplicity and good fitting (Seyssiecq et al., 2008). WAS also exhibits thixotropic behavior (Eshtiaghi et al., 2013; Farno et al., 2020), which means that the internal sludge structure is formed by a complex network based on the union of flocs and macroflocs that break down or build up slowly to adapt their structure to the applied shear. A common method to evaluate thixotropy is the hysteresis loop test, which consists of measuring the area enclosed between the up and down-curve of shear stress vs. shear rate over time (the called hysteresis area) when shear rate is linearly increased and decreased over time (Baudez, 2006; Tixier et al., 2003). However, the hysteresis area is a relative measurement of the thixotropy because it depends on the design parameters of the test and it is not a good parameter to compare the thixotropy of different samples with different viscosities (Baudez, 2006). Instead, thixotropy can be determined more accurately by means of a rheological structural model that defines the time evolution of a structural parameter, which is a numerical scalar measurement of the internal structure level, as a function of the kinetic coefficients for the breakdown and build-up processes (Moore, 1959). Accordingly, the major asset of this type of models is that the thixotropic behaviour is determined based on the magnitude of both kinetic coefficients instead of a relative measurement (the hysteresis area).

Limited information is available in the literature concerning rheological models to predict the thixotropic behaviour of WAS after applying a disintegration treatment. Ruiz-Hernando et al. (2015b) successfully implemented a rheological structural model to examine the variations of the thixotropic behaviour of WAS after thermal treatment. However, to the best of the authors' knowledge, this model has not yet been used to predict the thixotropy behaviour of WAS after ultrasound treatment. This is an important implication since the mechanism behind the disintegration of WAS flocs substantially differs between applying ultrasound or thermal treatment (Bougrier et al., 2006). These differences between ultrasound and thermal treatment can lead to high variations concerning the EPSs solubilisation mechanism with a direct impact on the rheological properties of the treated WAS. Accordingly, validating the rheological structural model for ultrasound treatment is crucial to understand its suitability to predict the variation of the thixotropic properties of ultrasonicated WAS.

The aim of the present study is to analyse the effect of the ultrasound treatment on the internal structure of the WAS and its underlying impact on EPSs solubilisation and dewatering properties. The rheological properties of the WAS have been analysed through the implementation of a rheological structural model and conducting creep tests. Finally, a techno-economic study has been conducted to evaluate the economic feasibility of ultrasound implementation for WAS pre-treatment before anaerobic digestion.

2. Materials and methods

2.1. Waste activated sludge samples

The thickened WAS samples used in this study were collected from a municipal wastewater treatment plant (WWTP) in the Barcelona metropolitan area (Spain) with a treatment capacity of 1,700,000 population equivalent. The sludge samples were stored at 4 °C until their utilisation. Detailed information of the main characteristics of the thickened WAS is provided in Table S1 of the supplementary information.

2.2. Ultrasound treatment conditions

The ultrasonic apparatus used was an HD2070 Sonopuls Ultrasonic Homogenizer equipped with a MS 73 titanium microtip probe (Bandelin, Berlin, Germany; 20 kHz). The ultrasonication power was fixed at 70 W and the exposure times were changed to provide a wide range of specific

energies (from 3000 to 33,000 kJ/kg TS), which were calculated following Eq. (1):

$$E_s = \frac{P \cdot t_a}{V \cdot TS} \quad (1)$$

where E_S is the specific energy applied (kJ/kg TS), P is the ultrasonic power of the ultrasonic homogeniser (kW), t_a is the application time (s), V is the sample volume (L), and TS is the concentration of total solids (kg/L).

Ultrasonication increases WAS temperature due to the thermal effect caused by the cavitation phenomenon (Pilli et al., 2011). Since the present study intended to solely analyse the effect of ultrasound treatment, it was necessary to nullify this thermal effect (Dewil et al., 2006). Accordingly, the beaker containing the samples was submerged in an ice bath to guarantee that the sludge temperature did not exceed 20 °C (Chu et al., 2001; Dewil et al., 2006).

2.3. Rheological characterisation

The rheometer used was a Haake RS300 control stress rheometer equipped with a temperature control system (thermostatic bath) and connected to a computer that allows programming the rheological assays and recording the data in real time (HAAKE Rheowin Software).

2.3.1. Hysteresis loop test, shear rate step test and rheological structural model theory

The rheological behaviour under flow conditions was analysed by the hysteresis loop and shear rate step tests. The sensor geometry used for both assays was a 4° cone and a flat stationary plate of 35 mm diameter. The average gap of the cone-plate geometry is 888 μm and the maximum centripetal acceleration at a shear rate of 300 s^{-1} (maximum shear rate applied) is 0.78 x g. Under such settings, the particles trapped in the gap and the movement of particles towards the edges is minimal. Measurements were conducted at 22 ± 0.1 °C and at a constant TS content (56.2 ± 0.4 g/kg). The hysteresis loop test was performed at two maximum shear rates (125 and 300 s^{-1}), following the procedure described by Ruiz-Hernando et al. (2014b). The shear rate step test consisted of pre-shearing the sludge at a fixed shear rate of 5 s^{-1} for 15 min and suddenly changing the shear rate to 30, 125 or 300 s^{-1} for 10 min to achieve steady states. The step tests were conducted in triplicate.

The variations in the thixotropic behaviour of WAS before and after the ultrasound treatment was analysed by means of a rheological structural model. The theory of the model has been extensively discussed in a previous study (Ruiz-Hernando et al., 2015b) and a summary of the equations used is provided in Table 1. The model is based on the definition of the structural parameter (S), which quantifies the structural level of the internal structure at any time and shear rate. Thereby, the value of S goes to zero when the internal structure is completely broken down (resulting in the lowest viscosity), while a complete build-up structure corresponds to the highest value of S (resulting in the highest viscosity). The breakdown and build-up of the internal network with shear-time is demonstrated with a constitutive equation (Eq. T1) and two kinetic equations (Eqs. T2.1 and T2.2), which consider the time dependence of the viscosity at constant shear rate conditions. On the other hand, WAS commonly behaves as non-Newtonian pseudoplastic fluid under steady state conditions. Accordingly, the steady state viscosity (η_e) was fitted to the Ostwald–de Waele model (Eq. T3.2).

2.3.2. Creep test

The rheological behaviour within the linear viscoelastic region was analysed by the creep test, following a similar procedure conducted in a previous study (Ruiz-Hernando et al., 2014b). Before starting the creep test, the sludge samples were kept at rest for 10 min to relax their structures. The limiting stress in the linear viscoelastic region was determined by conducting a shear sweep test from 0 to 200 Pa at a frequency of 1 Hz. The stresses that did not exceed 10 Pa assured that no changes were produced in the WAS internal structure. However, following a conservative criterion, the creep tests were conducted at 5 Pa. The compliance (strain divided by shear stress), $J(t)$, (Eq. (2)) was monitored for 15 min:

$$J(t) = \frac{\gamma(t)}{\tau_a} \quad (2)$$

where $\gamma(t)$ is the time-related strain (-) and τ_a is the applied shear stress (Pa).

The obtained compliance data were fitted to a Burgers model (Kelvin-Voigt cell in series with a Maxwell component), using Eq. (3):

$$J(t) = J_0 + J_m\left[1 - exp\left(\frac{-t}{\lambda}\right)\right] + \frac{t}{\eta_0} \quad (3)$$

where J_0 is the instantaneous elastic compliance of the Maxwell spring (Pa^{-1}); J_m is the viscoelastic compliance (Pa^{-1}) associated to the mean relaxation time (s) of the Kelvin–Voigt element; and η_0 is the zero-shear rate viscosity of the Maxwell dashpot (Pa·s).

A serrated plate-plate sensor geometry (35 mm in diameter) was used to avoid slipping of the sample in contact with the sensor. The sample was isolated from the environment to prevent evaporation of water from the sample during the test and measurements were conducted at 22 ± 0.1 °C.

Table 1
Summary of the equations used in the rheological structural model (Ruiz-Hernando et al., 2015b).

Constitutive equation for a pseudoplastic fluid:	
$\eta = S \cdot \dot{\gamma}^{-m}$	(T1)
Kinetic equations:	
$\frac{dS}{dt} = -K_{down} \cdot (S - S_e)$	(T2.1)
$\frac{dS}{dt} = -K_{up} \cdot (S - S_e)$	(T2.2)
At steady state conditions	
Constitutive equation:	
$\eta_e = S_e \cdot \dot{\gamma}^{-m}$	(T3.1)
Ostwald-de Waele equation:	
$\eta_e = a \cdot \dot{\gamma}^{n-1}$	(T3.2)
Structural parameter by combining Eqs. T3.1 and T3.2:	
$S_e = a \cdot \dot{\gamma}^{n+m-1}$	(T3.3)
The time evolution of viscosity is equal to the time evolution of structural parameter	
When shear rate is increased:	
$\frac{\eta - \eta_e}{\eta_i - \eta_e} = \frac{S - S_e}{S_i - S_e} = \exp(-K_{down} \cdot t)$	(T4.1)
When shear rate is decreased:	
$\frac{\eta - \eta_e}{\eta_i - \eta_e} = \frac{S - S_e}{S_i - S_e} = \exp(-K_{up} \cdot t)$	(T4.2)
Thixotropic kinetic coefficients depend on the shear rate in accordance with a potential equation	
$K_{down} = \alpha_{down} \cdot \dot{\gamma}^{\beta_{down}}$	(T5.1)
$K_{up} = \alpha_{up} \cdot \dot{\gamma}^{\beta_{up}}$	(T5.2)

2.4. EPSs extraction protocol

LB-EPSs and TB-EPSs were extracted following the procedure described by Ruiz-Hernando et al. (2015a). Briefly, the WAS sample was dewatered by centrifugation at 2000 x g for 10 min. The supernatant was collected for protein analysis and the bottom sediment was resuspended to the original volume using a buffered solution (pH 7). A mild method based on centrifugation (5000 x g for 15 min) was used for LB-EPSs extraction (Sheng et al., 2010). Subsequently, a harsh method based on ultrasonication followed by centrifugation (20,000 x g for 20 min) was applied for the TB-EPSs extraction.

2.5. Analytical methods

The soluble protein concentration of the supernatant obtained after the first centrifugation of the EPSs extraction protocol was analysed following the Lowry et al. (1951) method. Bovine serum albumin (BSA) was used as the standard and the absorbance was read at 750 nm using a UV/VIS spectrophotometer (Lambda 20, Perkin Elmer). The molecular weight distributions (MWD) of the LB-EPSs and TB-EPSs fractions were analysed by gel permeation chromatography (GPC) using a Waters Alliance 2695 chromatograph coupled to Waters 2996 photo diode array (PDA) detector (190–650 nm). The EPS fingerprints were analysed at 280 nm because proteins readily absorb at this wavelength due to their conjugated nature (Ras et al., 2011). Two serially linked columns (Ultrahydrogel 500, 10 μm, 7.8 × 300 mm and Ultrahydrogel 250, 6 μm, 7.8 × 300 mm) were used to obtain a wide selective permeation range and the molecular weight (MW) calibration was performed using five protein-like substances as standards (with MW from 197 to 200,000 Da). The detailed specifications of the GPC analysis can be found in Ruiz-Hernando et al. (2015a). All the samples were filtered through 0.45 μm low protein binding PVDF membranes.

The Capillary Suction Time (CST) was measured using a Type 304 M CST (Triton Electronics Ltd. UK). The bound water content was determined by calculating the difference between the total water content (measured by drying the sample at 105 °C) and the free water measured by Differential Scanning Calorimetry (DSC). This procedure assumes that bound water does not freeze at temperatures below the normal freezing point of water. Briefly, a weighted amount of sludge was added to the thermal analyser (Mettler Toledo DSC 30) with pure N_2 as the carrying gas. The temperature of the sludge sample was first decreased at a rate of 2 °C/min from 25 °C to −40 °C and then raised back to 40 °C at the same rate. The phase transition from water to ice was assumed to correspond to free water (Erdincler and Vesilind, 2003). Finally, the bound water content was expressed as kg bound water/kg TS. TS and volatile solid (VS) contents were measured in triplicate following the standard method 2540 G (APHA, 2005).

2.6. Economic analysis

A theoretical techno-economic analysis was conducted to evaluate the economic feasibility to implement an ultrasound reactor in a WWTP. Fig. S1 of the supplementary information illustrates the two scenarios considered for the economic analysis: (i) Baseline Scenario, where the ultrasound reactor was not implemented and (ii) Scenario 1, where the ultrasound reactor was implemented for WAS pre-treatment. The WAS production for the different scenarios was calculated considering that a theoretical WWTP treated 100,000 m^3/day of wastewater containing a chemical oxygen demand (COD) and nitrogen concentrations of 700 mg COD/L and 56 mg N/L, respectively (Vinardell et al., 2021a). The WWTP implemented a primary settler and a modified Ludzack-Ettinger configuration. The thickened WAS composition was based on the average of seven different sludges reported in the literature (Astals et al., 2013).

The methane production, solids removal and release of nutrients from thickened WAS anaerobic digestion were calculated considering steady-state equations for a continuous stirred tank reactor (CSTR). Detailed information on the steady-state equations used to model the anaerobic digester performance can be found in Vinardell et al. (2021a). The biodegradability and hydrolysis constant for the anaerobic digestion of thickened WAS and ultrasonicated WAS were obtained from Ruiz-Hernando et al. (2014a). The anaerobic digestion performance was modelled considering an organic loading rate of 1 kg VS/m^3/day.

The capital and operating costs influenced by the implementation of an ultrasound system were considered in this economic evaluation. Table S2 of the supplementary information shows detailed information of the parameters used for the cost calculations. The capital cost of the ultrasound reactor was considered to be 7500 €/kW based on previous data for full-scale ultrasound reactor configured as a double-tube reactor (Lippert et al., 2021). An specific energy input of 200 kJ/kg TS was considered for the ultrasound reactor, since it has been reported in full-scale ultrasound systems (Lippert et al., 2021). Ultrasound reactors usually need frequent replacement due to cavitation erosion (Pérez-Elvira et al., 2006). The lifetime of the ultrasound reactor was considered to be 3 years, which is comprised between the 1–6 years lifetime range evaluated by Lippert et al. (2021). It is worth mentioning that the specific energy input used in the present study (27,000 kJ/kg TS) was not considered in the economic analysis since this would not be a feasible option for full-scale ultrasound implementation (Lippert et al., 2021).

Electricity was generated from the biogas by using a combined heat and power (CHP) unit. The electrical efficiency of the CHP unit was 33% (Riley et al., 2020). The heat recovered in the CHP unit was used to keep the digester at 35 °C. An average electricity price of 0.1149 €/kWh was considered (Eurostat, 2019). The upgrading of the CHP system was necessary to adapt the existing CHP system to the increased biogas production after ultrasound implementation (Scenario 1). A unit cost of 712 €/kW_{el} was considered for the CHP system upgrading (Riley et al., 2020). An operating cost for the CHP system of 0.0119 €/kWh_{el} was used in the economic evaluation (Riley et al., 2020).

The digestate after anaerobic digestion was dewatered by centrifugation. Polyelectrolyte was dosed at 9 kg/t TS at a unit cost of 2.35 €/kg (Pretel et al., 2014; Vinardell et al., 2021a). An energy consumption of 0.045 kWh/kg TSS was considered for dewatering (Pretel et al., 2014). The biosolids (solid fraction of the centrifuge) were used in agriculture at a cost of 147 €/t TS (Vinardell et al., 2021a). The nutrients backload of the centrate (liquid fraction of the centrifuge) were treated in the mainstream of the WWTP. An energy consumption of 2.38 kWh/kg N was considered for nitrogen removal (Horstmeyer et al., 2018). Ferric chloride consumption for phosphorus precipitation was estimated from Taboada-Santos et al. (2020).

The capital expenditure (CAPEX), operating expenditure (OPEX) and electricity revenue were calculated for the two scenarios. Eq. (4) was used to calculate the net cost as the difference between the gross cost (annualised CAPEX + OPEX) and electricity revenue (Vinardell et al., 2021b).

$$\text{Net cost } (€/\text{y}) = \frac{i\cdot(1+i)^t}{(1+i)^t-1}\cdot CAPEX + OPEX - ER \quad (4)$$

where *CAPEX* is the capital expenditure (€), *OPEX* is the operating expenditure (€/year), *ER* is the electricity revenue (€/year), *t* is the project lifetime (years) and *i* is the discount rate (5%).

3. Results and discussion

3.1. Effect of the ultrasound treatment on the internal structure of the WAS

Table 2 shows the bound water content, CST and soluble protein content of the treated and untreated WAS samples for each ultrasound E_s

Table 2
Bound water content, CST and soluble protein-like substances concentration.

E_S (kJ/kg TS)	Bound water (kg/kg dry sludge)	CST (s)	Soluble protein content (mg/L)[1]
0	3.06	1562	416
3000	3.05	2454	1354
7000	3.11	2986	2158
17,000	3.46	4250	2974
27,000	3.83	6236	3740
33,000	4.06	[2]	4200

[1] Protein measurement on the supernatant resulting after centrifugation at 2000 g for 10 min.
[2] Value too high to be registered.

evaluated. It is worth mentioning that bound water is considered a gross estimate of several states of water including vicinal water (physically bound to solid particles surface by adsorption and adhesion), water of hydration (chemically bound to the solid particles) and a fraction of interstitial water (trapped within the floc structure or within a bacterial cell) (Erdincler and Vesilind, 2003). The results show that all the parameters increase as the ultrasound E_s increases, which indicates that the physicochemical characteristics in the internal structure of the WAS changed. The ultrasound treatment increased the soluble protein content over 100% for all the E_S analysed in comparison with the untreated sludge. This suggests that a large quantity of EPSs were released into the liquid phase since the soluble protein content, which is the major constituent of the EPSs, provides a reliable approximation of the degree of floc disruption and solubilisation (Guo et al., 2020; Li and Yang, 2007; Ruiz-Hernando et al., 2015a). From these results, it is conceivable to state that the EPSs released after sludge floc disruption increased the available surface for the physical binding of vicinal water, thus increasing the bound water content and hindering sludge dewatering. This is consistent with the results obtained for the CST test, which shows an increase up to 6236 s for an E_S of 27,000 kJ/kg TS. In the literature, it is widely accepted that high ultrasound E_S deteriorates sludge dewatering because it sharply increases the CST (Feng et al., 2009). Nevertheless, in a previous study it was found that a high ultrasound E_S (27,000 kJ/kg TS) improved WAS dewatering by centrifugation, although the CST increased. This was attributed to the release of the interstitial water trapped within sludge flocs and part of the vicinal water (Ruiz-Hernando et al., 2014b). Accordingly, it is conceivable that vicinal water was transferred to the supernatant together with colloidal and hydrophilic organic material.

Fig. 1 shows the MWD of LB-EPSs and TB-EPSs fractions for untreated and ultrasonicated WAS at 27,000 kJ/kg TS. In the present study, molecular weights equal or above the size of insulin (≥ 5800 Da) were considered proteins, whereas those below 5800 Da were considered protein building blocks (Lin et al., 1998). For the untreated WAS, most of the protein-like substances were found in the TB-EPS fraction (the innermost layer) and a very small amount was found in the LB-EPS fraction (the outermost layer). The ultrasound treatment solubilised a portion of the peptides and low-molecular-weight proteins, as evidenced by the increase in the LB-EPS fraction. Accordingly, it is conceivable that the ultrasound treatment caused structural changes in the WAS that can be attributed to two mechanisms: (i) disruption of the sludge flocs, which caused a reduction in size of sludge particles and increased the specific surface area for water attachment (Bougrier et al., 2006; Ruiz-Hernando et al., 2014b), and (ii) solubilisation of the low molecular weight EPSs, which changed the physicochemical characteristics of the WAS, such as turbidity, viscosity and surface charge, among others (Li et al., 2018).

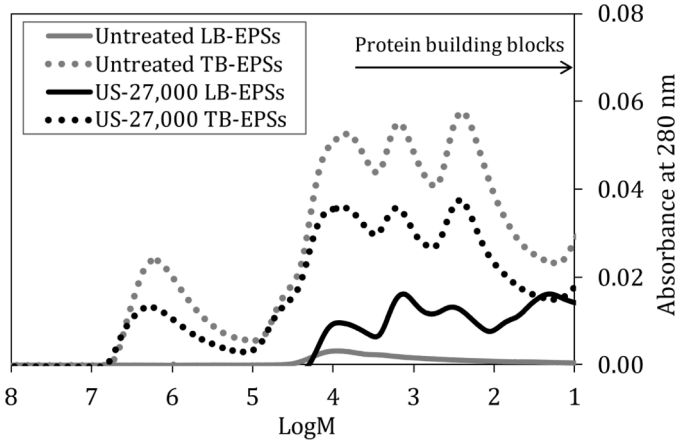

Fig. 1. Molecular size distribution of proteins in LB-EPS and TB-EPS fractions of untreated and ultrasonicated sludge (US) at 27,000 kJ/kg TS.

3.2. *Rheological structural model to quantify the thixotropic behaviour of WAS*

The rheological characterisation within the non-linear viscoelastic region was analysed by means of a rheological structural model. Fig. 2 illustrates the steady state viscosity as a function of shear rates between 5 and 300 s^{-1}. The results show that the untreated and ultrasonicated WAS (from 3000 to 33,000 kJ/kg TS) exhibited pseudoplastic behaviour, which means that the steady state viscosity decreased with the shear rate following a power law equation (Eq. T3.2). The Ostwald-de Waele model reproduced properly the pseudoplastic response of both the untreated and ultrasonicated WAS samples. The steady state viscosity was substantially reduced with the increase of the ultrasonic E_S applied. Specifically, for a shear rate of 300 s^{-1}, the steady state viscosity of the WAS treated at an E_S of 33,000 kJ/kg TS was reduced about 60%. This is mainly because the ultrasound treatment changed the internal structure of WAS, which affected its thixotropic behaviour.

The thixotropic kinetic coefficients for the breakdown process (K_{down}) were obtained from the step tests, following Eq. T4.1. Fig. 3a shows the K_{down} data as a function of the E_S applied for the three tested shear rates (30, 125 and 300 s^{-1}). The results show that K_{down} decreased when both the ultrasound E_S and shear rate increased, which means that the internal structure took more time to reach the steady state value. The reduction of K_{down} with ultrasound E_S was mainly observed at low shear rates (30 s^{-1}), whereas at high shear rates (125 and 300 s^{-1}) the K_{down} values remained relatively constant regardless of the E_S applied. This is because K_{down} depends on the shear rate in accordance with a potential equation (Eq. T5.1), from which the kinetic parameters for the breakdown process, α_{down} and β_{down}, can be obtained. Table 3 shows the α_{down} and β_{down} values with regression coefficient higher than 0.98. The negative value of β_{down} parameter means that the time to reach the equilibrium was higher at high shear rates. The shear rate dependency (observed by the values of $\beta_{down} \neq 0$) was slightly minimised as the ultrasound E_S was increased.

The alignment and deformation of sludge flocs to the applied shear rate (quantified by means of the m parameter) and the kinetic parameters for the build-up process (α_{up} and β_{up}) were obtained from the loop data, i.e., these parameters were varied to match the theoretical and experimental data using the steady state (a and n, obtained from the equilibrium data) and kinetic breakdown (α_{down} and β_{down}, obtained from the step data) parameters. In this context, the mathematical coupling effect among the adjusted parameters was reduced. The experimental data of the two loop tests (maximum shear rates of 125 and

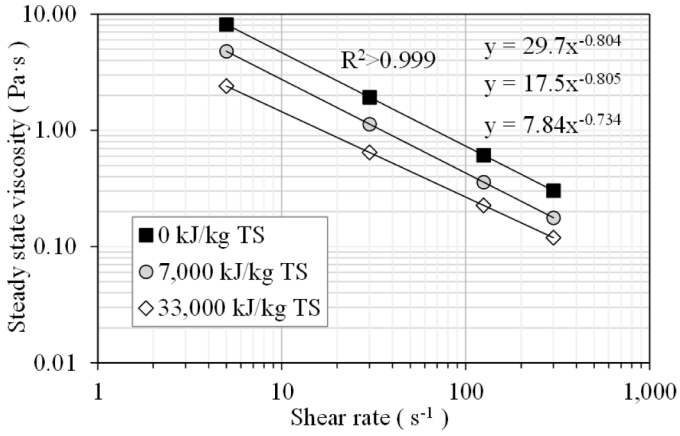

Fig. 2. Steady state viscosity as a function of shear rate (represented on a double-logarithmic scale) for the untreated and two ultrasonicated sludge samples (R^2> 0.999). The solid lines correspond to the fit to the Ostwald-de Waele power-law model (Eq. T3.2).

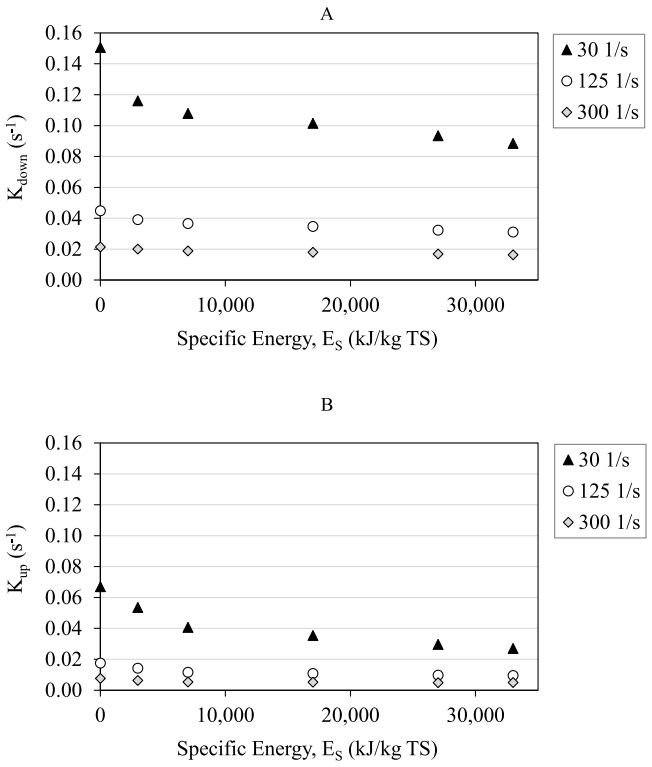

Fig. 3. Kinetic coefficients for (A) breakdown and (B) build-up processes for the untreated and ultrasonicated sludge samples at 30, 125 and 300 s^{-1}.

Table 3
Alignment and kinetic parameters for the breakdown and build-up processes.

E_S (kJ/kg TS)	α_{down} ($s^{\beta down-1}$)	β_{down} (-)	R^2[1]	m (-)[2]	α_{up} ($s^{\beta up-1}$)[2]	β_{up} (-)[2]	ARE (-)
0	2.695	−0.848	0.994	0.622	1.641	−0.940	0.148
3000	1.542	−0.761	0.985	0.604	1.246	−0.925	0.105
7000	1.418	−0.757	0.987	0.593	0.805	−0.877	0.132
17,000	1.308	−0.752	0.988	0.590	0.594	−0.829	0.238
27,000	1.172	−0.743	0.988	0.580	0.423	−0.781	0.160
33,000	1.070	−0.733	0.991	0.573	0.328	−0.733	0.226

[1] Correlation coefficients for the kinetic parameters for the breakdown process.

[2] These parameters where obtained by minimising the average relative error (ARE) between the experimental and calculated loop data.

300 s^{-1}) were fitted simultaneously by minimising the average relative error (ARE) between the experimental and calculated loop data. Fig. 4 shows the hysteresis loops for the untreated and ultrasonicated WAS. Table 3 shows the *m* parameter and the kinetic parameters of the build-up process (α_{up} and β_{up}) that better adjusted the experimental loop data (ARE<0.24). The results show that the *m* parameter slightly decreased as the E_S increased (Table 3). This means that the effect of the alignment or shape of aggregates (elastic deformation) at the new shear rate was more noticeable for less disrupted WAS structures (large structures) because of the lower E_S applied. The thixotropic kinetic coefficients for the build-up process (K_{up}) were calculated using Eq. T5.2 and considering the α_{up} and β_{up} parameters obtained from the loop data. As can be observed, K_{up} values (Fig. 3b) were always lower than K_{down} (Fig. 3a), which means that building up structures is a slower process than the breaking down.

All the sludges displayed positive thixotropic behaviour, which means that the shear stresses during the up-curves are higher than those at the same shear rate during the down-curves. The hysteresis area noticeably decreased when increasing ultrasound E_S (Fig. 4). This may

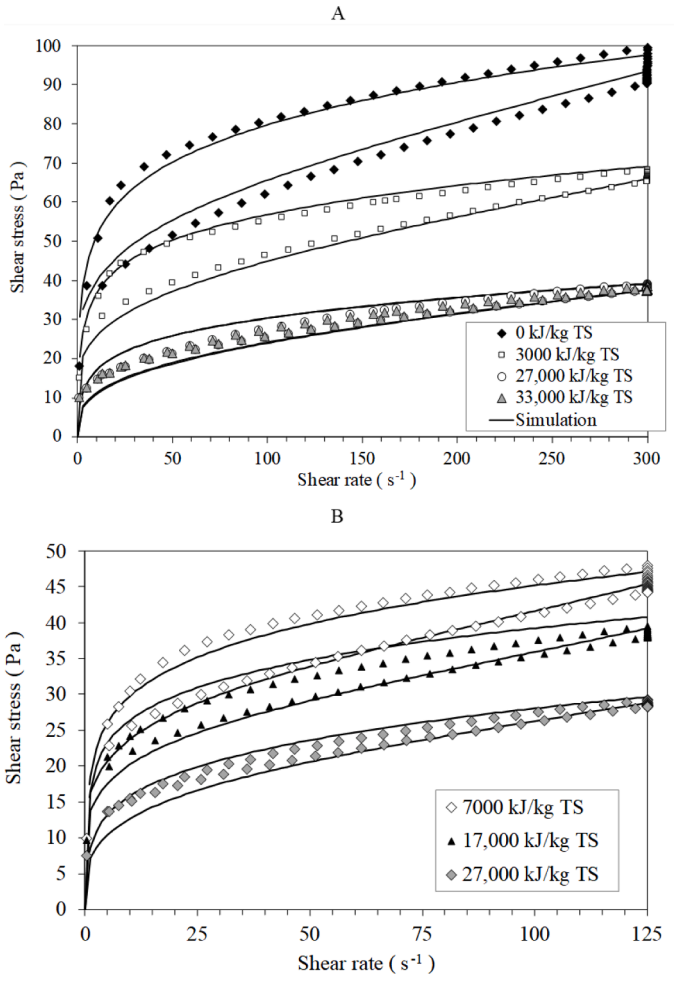

Fig. 4. Hysteresis loops obtained for the untreated and ultrasonicated sludge samples at a maximum shear rate of (A) 300 s^{-1} and (B) 125 s^{-1}. Solid lines correspond to the data predicted using the proposed model (Eqs. T1–T5.2).

seem to disagree with the theoretical results obtained with the model, since a large value of the hysteresis area might suggest a higher thixotropy (and vice versa). However, the hysteresis area is not a good parameter to compare the thixotropy of sludges with different viscosities, as in the case of ultrasonicated WAS samples (Baudez, 2006; Ruiz-Hernando et al., 2015b).

3.3. *Comparison of the viscoelastic behaviour between untreated, ultrasonicated and dewatered WAS*

The creep test was conducted for the untreated, ultrasonicated at 27,000 kJ/kg TS and dewatered WAS. The dewatered WAS was obtained by centrifugation of the ultrasonicated sludge (27,000 kJ/kg TS), followed by the removal of the bulk water by decantation. The reason for choosing 27,000 kJ/kg TS was because this E_S allowed a reduction in shear stress (and therefore the viscosity) similar to the maximum ultrasound E_S applied (33,000 kJ/kg TS) (Fig. 4a). Fig. 5a shows the creep compliance data corresponding to the untreated, ultrasonicated and dewatered sludge samples, and their respective best fits to the Burgers model (Eq. (3)). The good fit of the experimental data demonstrated the capability of the Burgers model to reproduce the viscoelastic response of the sludges. The compliance data for the three sludges exhibited the typical evolution of a viscoelastic material, which implies three different behaviours in time: (i) an initial sudden increase of the compliance (which corresponds to a pure elastic behaviour), (ii) an increase at a variable rate (which corresponds to a viscoelastic behaviour), and (iii)

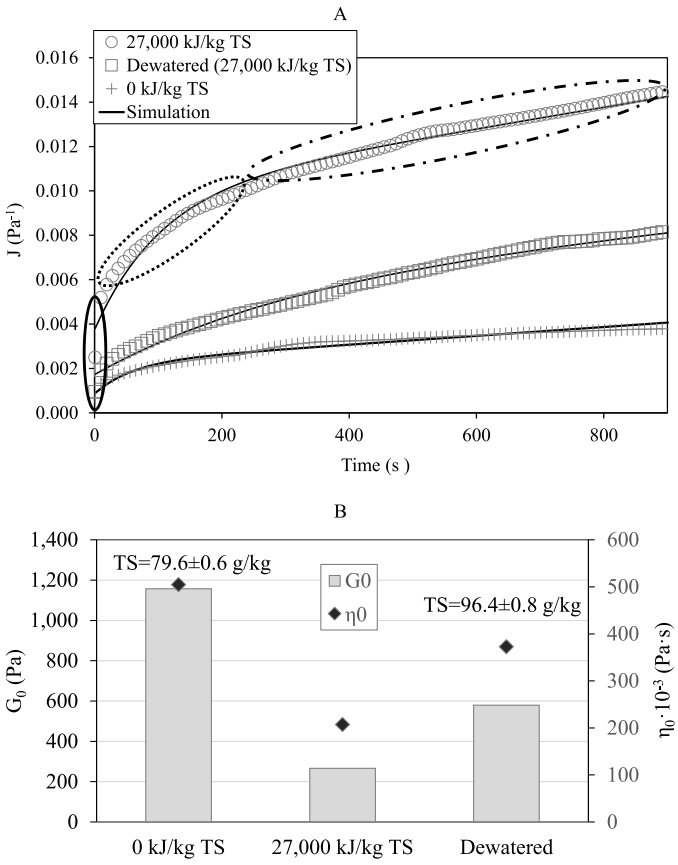

Fig. 5. Creep assay for the untreated, ultrasonicated at 27,000 kJ/kg TS and dewatered sludges. (A) Creep compliance data (the solid black lines correspond to the best fit to the model described in Eq. (3)). The three behaviours in time have been indicated with ellipses for the ultrasonicated sludge (the continuous line refers to the pure elastic behaviour, the dotted line refers to the viscoelastic behaviour and the mixed line refers to the pure viscous behaviour). (B) Initial elasticity (G_0) and zero shear rate viscosity (η_0).

an increase at a constant rate (which corresponds to a pure viscous behaviour). The ultrasonicated sludge exhibited the highest values of compliance, followed by the dewatered and untreated sludges. Accordingly, ultrasonicated sludge was more easily deformed by a given stress. The pure elastic behaviour can be quantified with the parameter G_0, which measures the initial elasticity of the sample and corresponds to the inverse of J_0. On the other hand, the pure viscous behaviour can be quantified with the parameter η_0, which corresponds to the zero-shear rate viscosity (Moreira et al., 2010). Both parameters (G_0 and η_0) were obtained with the model described in Eq. (3) and are shown in Fig. 5b. The untreated sludge exhibited the highest values of (i) G_0, which indicates that it is formed by mechanically strong and rigid structures, and (ii) η_0, which indicates that these structures are large. Conversely, the sludge treated at 27,000 kJ/kg TS exhibited the lowest G_0 and η_0 values, which means that the ultrasound treatment loosened and disrupted the internal structure of the WAS. Fig. 5b also shows the TS content of the untreated and dewatered sludges. Specifically, dewatered sludge resulted in an increase of approximately 21% of the TS content in comparison with the untreated sludge. Nevertheless, despite being more concentrated, the dewatered sludge exhibited a reduction in the zero-shear rate viscosity, thus being easier to handle than the untreated sludge. Finally, the viscoelastic behaviour can be quantified with the parameters of the Kelvin-Voigt element, i.e., (i) the relaxation time of a structure (λ), which is closely related to the size of the structure, and (ii) the elasticity modulus ($G_m = 1/J_m$), which is related to the number of these structures (Llorens et al., 2003). Specifically, the G_m values were 705 Pa for the untreated sludge, 162 Pa for the ultrasonicated sludge at 27,000 kJ/kg TS, and 238 Pa for the dewatered sludge, which means that the ultrasound treatment decreased the number of structures in the relaxation time analysed.

3.4. Economic analysis

3.4.1. Economic feasibility to implement an ultrasound reactor in a WWTP

Fig. 6 shows the economic results to implement an ultrasound reactor to pre-treat WAS in a theoretical WWTP. The results show that the implementation of an ultrasound reactor is not yet economically favourable since the Baseline Scenario featured a net cost lower than Scenario 1. In Scenario 1, ultrasound implementation led to an increase in electricity revenue and a reduction in the amount of solids to be managed as a result of the higher solids degradation in the anaerobic digester. However, these economic incomes did not offset the higher capital and operating costs of the ultrasound reactor, which is the main reason why Scenario 1 featured a net cost (764,485 €/year) 14% higher than the Baseline Scenario (668,081 €/year). Besides economic considerations, the implementation of an ultrasound reactor can facilitate WAS management due to its reduced viscosity (Lippert et al., 2021).

3.4.2. Sensitivity analysis

Fig. 7 shows the sensitivity analysis of the Baseline Scenario and Scenario 1. The sensitivity analysis was performed by changing ±30% the base case value considered for the economic analysis. The sensitivity analysis is a useful tool to evaluate the key economic drivers affecting the economics of the process (Li et al., 2020). It is worth mentioning that costs that did not experience variation because they solely depended on ultrasound implementation have not been illustrated for the Baseline Scenario. The results show that biosolids disposal cost had the highest impact on the net cost of both scenarios. In the Baseline Scenario, the net cost variation caused by biosolids disposal cost was higher than in Scenario 1 since Scenario 1 produced a lower amount of biosolids due to its higher solids reduction in the anaerobic digester. Electricity price also had a high impact on net cost because an increase or reduction of this parameter impacted the revenue achieved from electricity production. Unlike biosolids disposal cost, the net cost variation caused by electricity price was higher in Scenario 1 than in the Baseline Scenario since Scenario 1 produced a higher amount of electricity after the implementation of an ultrasound system. These results suggest that further improvements in WAS biodegradability through ultrasonication are important to improve the competitiveness of ultrasound systems. This idea was reinforced observing the results of the sensitivity analysis,

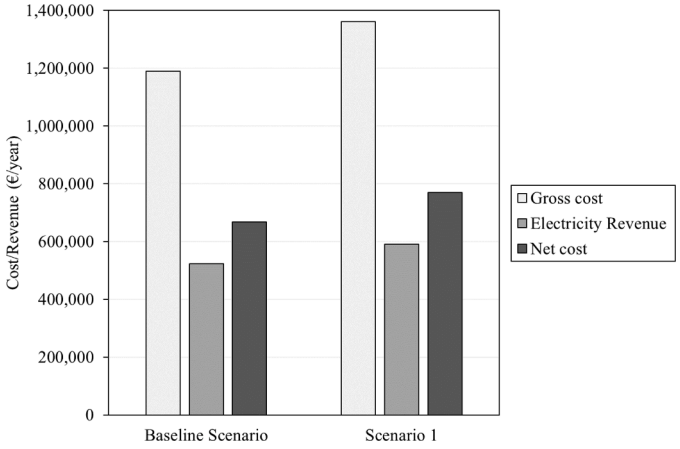

Fig. 6. Gross cost, electricity revenue and net cost for the Baseline Scenario (without ultrasonication) and Scenario 1 (implementing ultrasonication). The net cost (dark bar) resulted from the difference between the gross cost (white bar) and electricity revenue (grey bar).

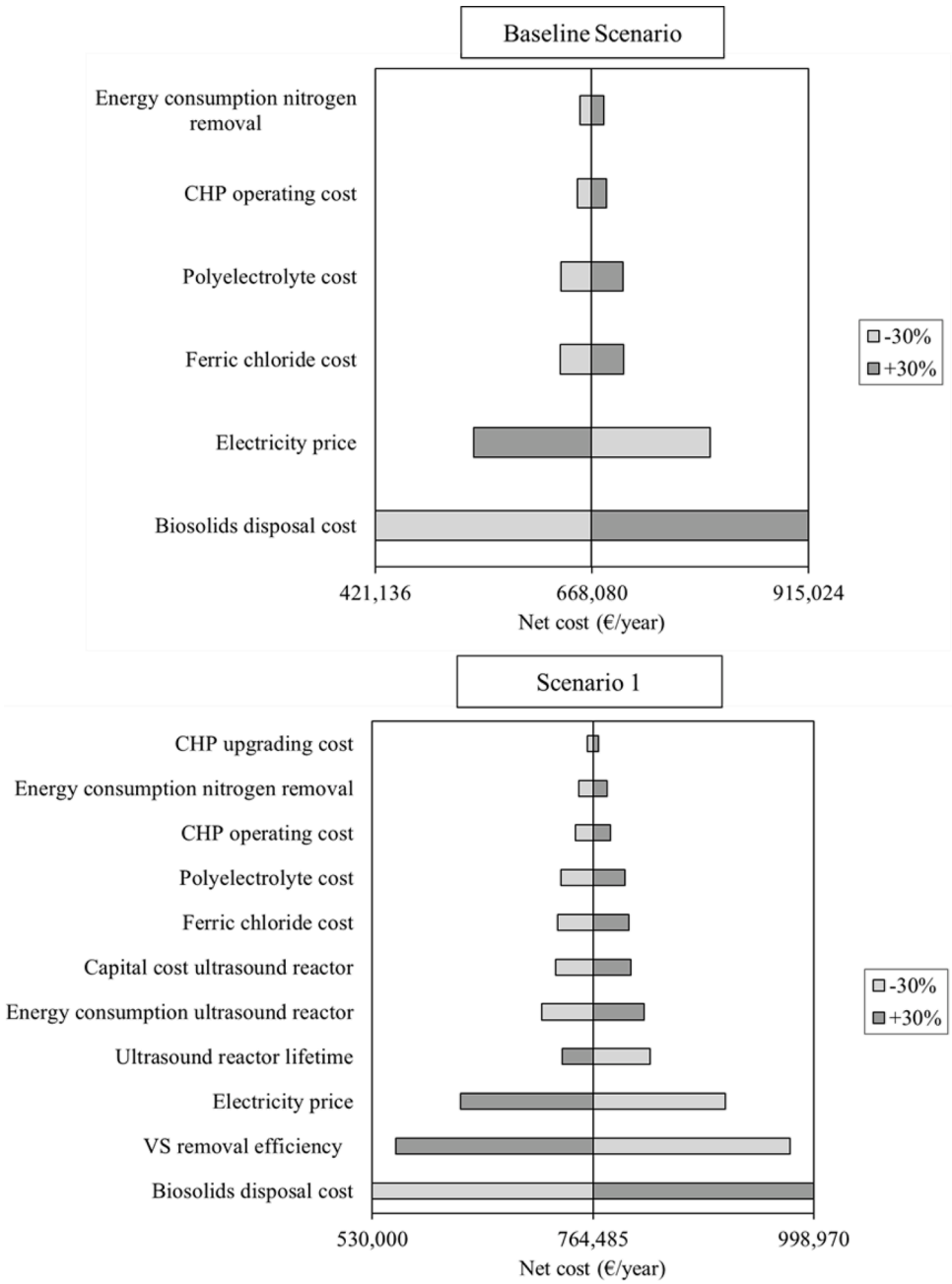

Fig. 7. Sensitivity analysis for $a \pm 30\%$ variation of the parameters of (top) Baseline Scenario (without ultrasonication) and (bottom) Scenario 1 (implementing ultrasonication).

which show that increasing the VS removal efficiency from ultrasonicated WAS anaerobic digestion could make Scenario 1 more competitive than the Baseline Scenario (Fig. 7). Specifically, Scenario 1 should achieve a methane production increase of 30% (only including WAS in the mass balance) from ultrasonicated WAS anaerobic digestion to outcompete the Baseline Scenario. This means that a total methane production increase of 12% (including WAS and primary sludge (PS) in the mass balance) would be necessary for an anaerobic digester initially treating mixed PS and WAS (50% PS and 50% WAS on VS-basis). These results show that ultrasound implementation could be economically competitive since increments in total methane production above 15% have been reported in full-scale anaerobic digesters treating PS and ultrasonicated WAS (Hogan et al., 2004; Xie et al., 2007). However, it is worth mentioning that the costs of the ultrasound equipment have been calculated considering a novel double-tube ultrasound reactor operated at a relatively low energy input of 200 kJ/kg TS (Lippert et al., 2021). In their study, Lippert et al. (2021) observed that this reactor configuration reduced clogging risk in comparison to more typical ultrasound reactors such as sonotrode or radial horn with a direct impact on the ultrasound reactor lifetime. However, the authors only reported a slight increase in methane production of 6.2% (statistically not significant) for this configuration that was primarily attributed to the low ultrasonic density in comparison to full-scale sonotrode and radial horn reactors as well as to the low efficiency of the double-tube reactor when treating high-solid content streams such as WAS. From the results reported by Lippert et al. (2021), it does not appear possible to reach total methane production increases of 12% considering the current development of the double-tube reactor configuration. Therefore, the results obtained in the present study should be further expanded considering other reactor configurations. Importantly, these studies should also include the

impact of reactor configuration on ultrasound system integrity since it could play a key role in the total operating costs. Overall, the economic and technical competitiveness of an ultrasound system for WAS pre-treatment depends on its capacity to increase the biodegradability of WAS while keeping the system at a moderate risk of clogging and erosion.

4. Conclusions

This study evaluated the impact of ultrasound treatment on WAS rheology, dewatering properties and process economics. A rheological structural model was implemented to better understand the change of the WAS internal structure after ultrasound treatment. Ultrasound treatment disrupted the WAS flocs and solubilised a portion of the EPSs with a direct impact on the rheological and dewatering properties of WAS. However, the implementation of ultrasonication in a WWTP is not yet economically feasible. The main conclusions of this study are summarised as follows:

- Ultrasound treatment disrupted WAS flocs since the soluble protein content increased from 416 to 3740 mg/L as the ultrasound E_S increased from 0 to 27,000 kJ/kg TS. As a result, the bound water and the CST increased because the proteins increased the available surface for water attachment.
- The rheological structural model demonstrated that increasing ultrasound E_S reduced the kinetic coefficient for the breakdown process and changed the fast speed of alignment of flocs because of the reduction of WAS structures.
- The creep measurements performed within the linear viscoelastic region showed that the ultrasound treatment at an E_S of 27,000 kJ/kg TS reduced the initial elasticity and the zero-shear rate viscosity by approximately 80% and 60%, respectively, which means that the internal structure of the WAS loosened and disrupted.
- The ultrasonicated and dewatered sludge exhibited more complex networks due to the higher soluble protein content but exhibited a weak connection between internal structures since both the viscosity and the initial elasticity at rest decreased.
- The techno-economic analysis showed that ultrasound implementation was not yet economically attractive since its implementation featured a net cost about 14% higher than the scenario that did not implement ultrasonication. However, achieving an increase of 12% in methane production in an anaerobic digester initially treating WAS and PS could make ultrasound implementation economically attractive.

Declaration of Competing Interest

The authors declare that they have no known competing financial interests or personal relationships that could have appeared to influence the work reported in this paper.

Acknowledgments

The authors are grateful to the Spanish Ministerio de Ciencia e Innovacion (Project CTQ2009–11465) for funds received to carry out this study. Sergi Vinardell is grateful to the Generalitat de Catalunya for his predoctoral FI grant (2019 FI_B 00394). The authors are also thankful to EMSSA for providing samples and sampling facilities.

Supplementary materials

Supplementary material associated with this article can be found, in the online version, at doi:10.1016/j.watres.2021.117855.

References

APHA, 2005. Standard Methods for the Examination of Water and Wastewater. American Public Health Association, Washington.
Appels, L., Baeyens, J., Degrève, J., Dewil, R., 2008. Principles and potential of the anaerobic digestion of waste-activated sludge. Prog. Energy Combust. Sci. 34, 755–781.
Astals, S., Esteban-Gutiérrez, M., Fernández-Arévalo, T., Aymerich, E., García-Heras, J.L., Mata-Alvarez, J., 2013. Anaerobic digestion of seven different sewage sludges: a biodegradability and modelling study. Water Res. 47, 6033–6043.
Bandelin, J., Lippert, T., Drewes, J.E., Koch, K., 2020. Assessment of sonotrode and tube reactors for ultrasonic pre-treatment of two different sewage sludge types. Ultrason. Sonochem. 64, 105001.
Baudez, J.C., 2006. About peak and loop in sludge rheograms. J. Environ. Manag. 78, 232–239.
Bougrier, C., Albasi, C., Delgenès, J.P., Carrère, H., 2006. Effect of ultrasonic, thermal and ozone pre-treatments on waste activated sludge solubilisation and anaerobic biodegradability. Chem. Eng. Process. Process Intensif. 45, 711–718.
Carrère, H., Dumas, C., Battimelli, A., Batstone, D.J., Delgenès, J.P., Steyer, J.P., Ferrer, I., 2010. Pretreatment methods to improve sludge anaerobic degradability: a review. J. Hazard. Mater. 183, 1–15.
Chu, C.P., Chang, B.V., Liao, G.S., Jean, D.S., Lee, D.J., 2001. Observations on changes in ultrasonically treated waste-activated sludge. Water Res. 35, 1038–1046.
Dewil, R., Baeyens, J., Goutvrind, R., 2006. Ultrasonic treatment of waste activated sludge. Environ. Prog. 25, 121–128.
Erdincler, A., Vesilind, P.A., 2003. Effect of sludge water distribution on the liquid-solid separation of a biological sludge. J. Environ. Sci. Heal. Part A Toxic/Hazard. Subst. Environ. Eng. 38, 2391–2400.
Eshtiaghi, N., Markis, F., Yap, S.D., Baudez, J.C., Slatter, P., 2013. Rheological characterisation of municipal sludge: a review. Water Res. 47, 5493–5510.
Eurostat, Electricity price statistics. https://ec.europa.eu/eurostat/statistics-explained/index.php/Electricity_price_statistics, 2019 (accessed 30 September 2019).
Farno, E., Lester, D.R., Eshtiaghi, N., 2020. Constitutive modelling and pipeline flow of thixotropic viscoplastic wastewater sludge. Water Res. 184, 116126.
Feng, X., Deng, J., Lei, H., Bai, T., Fan, Q., Li, Z., 2009. Dewaterability of waste activated sludge with ultrasound conditioning. Bioresour. Technol. 100, 1074–1081.
Gallipoli, A., Braguglia, C.M., 2012. High-frequency ultrasound treatment of sludge: combined effect of surfactants removal and floc disintegration. Ultrason. Sonochem. 19, 864–871.
Guo, H., Felz, S., Lin, Y., van Lier, J.B., de Kreuk, M., 2020. Structural extracellular polymeric substances determine the difference in digestibility between waste activated sludge and aerobic granules. Water Res. 181, 115924.
He, D., Xiao, J., Wang, D., Liu, X., Fu, Q., Li, Y., Du, M., Yang, Q., Liu, Y., Wang, Q., Ni, B. J., Song, K., Cai, Z., Ye, J., Yu, H., 2021. Digestion liquid based alkaline pretreatment of waste activated sludge promotes methane production from anaerobic digestion. Water Res. 199, 117198.
Hogan, F., Mormede, S., Clark, P., Crane, M., 2004. Ultrasonic sludge treatment for enhanced anaerobic digestion. Water Sci. Technol. 50, 25–32.
Horstmeyer, N., Weißbach, M., Koch, K., Drewes, J.E., 2018. A novel concept to integrate energy recovery into potable water reuse treatment schemes. J. Water Reuse Desalin. 8, 455–467.
Houghton, J.I., Stephenson, T., 2002. Effect of influent organic content on digested sludge extracellular polymer content and dewaterability. Water Res. 36, 3620–3628.
Labanda, J., Llorens, J., 2006. A structural model for thixotropy of colloidal dispersions. Rheol. Acta 45, 305–314.
Li, X., Guo, S., Peng, Y., He, Y., Wang, S., Li, L., Zhao, M., 2018. Anaerobic digestion using ultrasound as pretreatment approach: changes in waste activated sludge, anaerobic digestion performances and digestive microbial populations. Biochem. Eng. J. 139, 139–145.
Li, X.Y., Yang, S.F., 2007. Influence of loosely bound extracellular polymeric substances (EPS) on the flocculation, sedimentation and dewaterability of activated sludge. Water Res. 41, 1022–1030.
Li, Y., Han, Y., Zhang, Y., Luo, W., Li, G., 2020. Anaerobic digestion of different agricultural wastes : a techno-economic assessment. Bioresour. Technol. 315, 123836.
Lin, D.T., Cheng, L.P., Kang, Y.J., Chen, L.W., Young, T.H., 1998. Effects of precipitation conditions on the membrane morphology and permeation characteristics. J. Memb. Sci. 140, 185–194.
Lippert, T., Bandelin, J., Vogl, D., Alipour Tesieh, Z., Wild, T., Drewes, J.E., Koch, K., 2021. Full-scale assessment of ultrasonic sewage sludge pretreatment using a novel double-tube reactor. ES&T Eng. 1, 298–309.
Liu, X., Huang, X., Wu, Y., Xu, Q., Du, M., Wang, D., Yang, Q., Liu, Y., Ni, B.J., Yang, G., Yang, F., Wang, Q., 2020. Activation of nitrite by freezing process for anaerobic digestion enhancement of waste activated sludge: performance and mechanisms. Chem. Eng. J. 387, 124147.
Llorens, J., Rudé, E., Marcos, R.M., 2003. Polydispersity index from linear viscoelastic data: unimodal and bimodal linear polymer melts. Polymer 44, 1741–1750 (Guildf).
Lowry, O.H., Rosebrough, N.J., Farr, A.L., Randall, R.J., 1951. Protein measurement with the folin phenol reagent. J. Biol. Chem. 193, 265–275.
Moore, F., 1959. The rheology of ceramic slips and bodies. Trans. Br. Ceram. Soc. 58, 470–475.
Moreira, R., Chenlo, F., Torres, M.D., Prieto, D.M., 2010. Influence of the particle size on the rheological behaviour of chestnut flour doughs. J. Food Eng. 100, 270–277.
Pérez-Elvira, S.I., Nieto Diez, P., Fdz-Polanco, F., 2006. Sludge minimisation technologies. Rev. Environ. Sci. Biotechnol. 5, 375–398.

Pilli, S., Bhunia, P., Yan, S., LeBlanc, R.J., Tyagi, R.D., Surampalli, R.Y., 2011. Ultrasonic pretreatment of sludge: a review. Ultrason. Sonochem. 18, 1–18.
Pretel, R., Robles, A., Ruano, M.V., Seco, A., Ferrer, J., 2014. The operating cost of an anaerobic membrane bioreactor (AnMBR) treating sulphate-rich urban wastewater. Sep. Purif. Technol. 126, 30–38.
Radjenović, J., Petrović, M., Barceló, D., 2009. Fate and distribution of pharmaceuticals in wastewater and sewage sludge of the conventional activated sludge (CAS) and advanced membrane bioreactor (MBR) treatment. Water Res. 43, 831–841.
Ras, M., Lefebvre, D., Derlon, N., Paul, E., Girbal-Neuhauser, E., 2011. Extracellular polymeric substances diversity of biofilms grown under contrasted environmental conditions. Water Res. 45, 1529–1538.
Ratkovich, N., Horn, W., Helmus, F.P., Rosenberger, S., Naessens, W., Nopens, I., Bentzen, T.R., 2013. Activated sludge rheology: a critical review on data collection and modelling. Water Res. 47, 463–482.
Riley, D.M., Tian, J., Güngör-Demirci, G., Phelan, P., Rene Villalobos, J., Milcarek, R.J., 2020. Techno-economic assessment of CHP systems in wastewater treatment plants. Environments 7, 1–32.
Ruiz-Hernando, M., Cabanillas, E., Labanda, J., Llorens, J., 2015a. Ultrasound, thermal and alkali treatments affect extracellular polymeric substances (EPSs) and improve waste activated sludge dewatering. Process Biochem. 50, 438–446.
Ruiz-Hernando, M., Labanda, J., Llorens, J., 2015b. Structural model to study the influence of thermal treatment on the thixotropic behaviour of waste activated sludge. Chem. Eng. J. 262, 242–249.
Ruiz-Hernando, M., Martín-Díaz, J., Labanda, J., Mata-Alvarez, J., Llorens, J., Lucena, F., Astals, S., 2014a. Effect of ultrasound, low-temperature thermal and alkali pre-treatments on waste activated sludge rheology, hygienization and methane potential. Water Res. 61, 119–129.
Ruiz-Hernando, M., Simón, F.X., Labanda, J., Llorens, J., 2014b. Effect of ultrasound, thermal and alkali treatments on the rheological profile and water distribution of waste activated sludge. Chem. Eng. J. 255, 14–22.
Seyssiecq, I., Marrot, B., Djerroud, D., Roche, N., 2008. In situ triphasic rheological characterisation of activated sludge, in an aerated bioreactor. Chem. Eng. J. 142, 40–47.
Sheng, G.P., Yu, H.Q., Li, X.Y., 2010. Extracellular polymeric substances (EPS) of microbial aggregates in biological wastewater treatment systems: a review. Biotechnol. Adv. 28, 882–894.
Taboada-Santos, A., Rivadulla, E., Paredes, L., Carballa, M., Romalde, J., Lema, J.M., 2020. Comprehensive comparison of chemically enhanced primary treatment and high-rate activated sludge in novel wastewater treatment plant configurations. Water Res. 169, 115258.
Tixier, N., Guibaud, G., Baudu, M., 2003. Towards a rheological parameter for activated sludge bulking characterisation. Enzyme Microb. Technol. 33, 292–298.
Vinardell, S., Astals, S., Koch, K., Mata-Alvarez, J., Dosta, J., 2021a. Co-digestion of sewage sludge and food waste in a wastewater treatment plant based on mainstream anaerobic membrane bioreactor technology: a techno-economic evaluation. Bioresour. Technol. 330, 124978.
Vinardell, S., Dosta, J., Mata-Alvarez, J., Astals, S., 2021b. Unravelling the economics behind mainstream anaerobic membrane bioreactor application under different plant layouts. Bioresour. Technol. 319, 124170.
Weemaes, M.P.J., Verstraete, W.H., 1998. Evaluation of current wet sludge disintegration techniques. J. Chem. Technol. Biotechnol. 73, 83–92.
Xie, R., Xing, Y., Ghani, Y.A., Ooi, K.E., Ng, S.W., 2007. Full-scale demonstration of an ultrasonic disintegration technology in enhancing anaerobic digestion of mixed primary and thickened secondary sewage sludge. J. Environ. Eng. Sci. 6, 533–541.